Development and assessment of a quality assurance device for radiation field-light field congruence testing in diagnostic radiology

Jan Lindström, Markus Hulthen, Michael Sandborg and Åsa Carlsson Tedgren

Tweet

LIU LINKÖPING UNIVERSITY

Development and assessment of a quality assurance device for radiation field light field congruence testing in diagnostic radiology

Jan Lindström,[a,b] Markus Hulthén,[a] Michael Sandborg,[b] Åsa Carlsson Tedgren, [a,b]

[a]Department of Medical Radiation Physics and Nuclear Medicine, Karolinska University Hospital, Stockholm, Sweden
[b]Medical Radiation Physics, IMH and CMIV, Linköping University, Linköping, Sweden

Abstract.

Purpose: Existing methods for checking the light field radiation field congruence on x-ray equipment either do not fully meet the conditions of various quality control standards regarding inherent uncertainty requirements or contain subjective steps, further increasing the uncertainty of the end result. The aim of this work was to develop a method to check the light field radiation field congruence on all x-ray equipment. The result should have a low uncertainty which is accomplished by eliminating most subjective user steps in the method. A secondary aim was to maintain the same level of usability as of comparable methods but still able to store the result.

Approach: A new device has been developed where the light field and corresponding radiation field are monitored through measurements of the field edge locations (in total: 2 x 4 edges). The maximum field size location deviation between light field and radiation field in the new method, is constrained by the physical limitations of the sensors used in various versions of the prototype: Linear Image Sensors (LISs) of 25-29 mm active sensor length. The LISs were sensitized to x-rays by applying a phosphor strip of Gd_2O_2S:Tb covering the light sensor input area. Later prototypes of the completed LIS device also have the option of a Bluetooth (100 m range standard) connection, thus increasing the mobility.

Results: The developed device has a special feature of localization a field edge without any prior, subjective, alignment procedure of the user, i.e. the signals produced were processed by software storing the associated field edge profiles, localizing the edges in them, and finally displaying the calculated deviation. The uncertainty in field edge location difference was estimated to be less than 0.1 mm (k=2). The calculated uncertainty is lower than for other, commercially available, methods for light field radiation field congruence also presented in this work.

Conclusions: A new method to check the light field radiation field congruence of x-ray systems was developed to improve on the limitations found in existing methods, such as device detector resolution, subjective operator steps or the lack of storing results for later analysis. The development work overcame several challenges including mathematically describing real life edges of light and radiation fields, noise reduction of radiation edges and mapping/quantification of the rarely observed phenomenon of focal spot wandering. The assessment of the new method showed that the listed limitations were overcome, and the aims were accomplished. It is therefore believed that the device can improve the work in quality controls of x-ray systems.

Keywords: congruence; field edge; focal spot wandering; linear image sensor; radioluminescence; quality control

1 Introduction

Historically, the functions of x-ray equipment were checked only by service engineers during routine maintenance. Later, with the introduction of quality assurance systems, other professionals like radiologists, technologists, medical physicists etc. became involved in checking x-ray equipment. The aim was not only to maintain the functions, but also to systematically assess and optimize the balance between patient dose and image quality. One of the tests in quality assurance systems is the light field

radiation field congruence. The light field in x-ray equipment is used to position and restrict the radiation field to the area of diagnostic interest.[1] The task of determining the light field – radiation field (x-ray field) congruence, is a part of routine Quality Control (QC) checks for diagnostic x-ray equipment. A poor alignment between the two fields has negative consequences; not all anatomic structures of interest may be within the image boundaries and/or radiation sensitive organs may be unnecessarily irradiated.[2,3] Even though the control of the light field – radiation field congruence is an essential part of routine QC, only few studies have been published demonstrating the expected consequences noted above. One study has shown that a 2 cm offset in a chest exam may result in up to ±22% in exposure variations.[4] Another study indicated a 20% increase of the effective dose for two of three simulated clinical examinations performed at the maximum permissible level of deviation.[5] It is therefore a clear risk for an increased population dose if possible misalignments between the light and radiation field are not frequently checked and subsequently corrected for.

National and international standards on the maximum permissible deviation from the congruence between light and radiation field, base their limits on the calculation of the maximum sum of misalignments of 2% of the Source to Image detector Distance (SID) between the light and radiation field at two opposing field sides.[6,7] This applies to all x-ray equipment using a light field as an alignment and x-ray field adjustment feature.

The regular controls of the congruence usually involve manual alignment to an x-ray opaque marker or scale, positioned in the light field, hence using subjective, visual assessment. The marker then appears in the x-ray image showing any deviation from congruence. The subjectivity of this control was investigated by Kron and Ferguson (2000) for radiotherapy machine light fields.[8] They found a considerable variation between operators. Considering these findings and the variety of professions involved in Quality Assurance, an objective method of establishing the light field edge location (and corresponding x-ray field edge) would therefore be desirable.

There are dedicated tools for checking the congruence and their corresponding methods can be broken down into the following categories;

1) Field edge detection (needs in total four x-ray exposures for entire field and corresponding manual alignment of the light field edge position).

2) Entire field, utilizing fluorescence and/or phosphorescence in a square plane

3) Radiochromatic film i.e. a substance changing optical appearance following exposure (non-reversible).

There are several commercially available devices from these categories. Representatives from each category have been chosen in this work for a comparison with the newly developed method.

Central to this work is an in-house development of a novel, radioluminescence based quality control device for objective light field - radiation field congruence checks. A conference proceeding covering early parts of this work was presented in 2014 (SPIE).[9]

A similar approach, but for light field edges only, was presented by Bottaro et al (2017).[10]

The novel device is based on a one-dimensional Linear Image Sensor (LIS). The denotation, "LIS-method", is therefore used for the developed device throughout the rest of this work. The LIS-method belongs to method category 1, as described earlier, i.e. edge detection.

The aim of this work is to develop a method capable of displaying deviations equal or smaller to the strictest standards for the light field - radiation field congruence and at the same time improve on the inherent uncertainty of the currently available methods. To further improve on existing, comparable methods, additional aims were to eliminate subjective steps i.e. manual alignment of light field edge by sight and the step of keying in or manually writing down the measurement result. With the variety of end users in mind (maintenance engineers, physicists, radiologists, technicians etc.), a requirement was the new method should not entail extra time and effort to obtain the results. Another useful

possibility would be to store the results for later analysis on a PC. There is a variety of possible demands for keeping a record of the measurements in a Quality Assurance system. But normally all results should be kept until at least the next measurement session. They should also be readily available if a national authority performs an inspection.

2   Methods and Materials

An overview of field and edge definitions is provided in Section 2.1. The LIS-method is based on existing LIS camera OEM (Original Equipment Manufacturer) boards and their associated software. The development steps include modifications to the basic hardware and are described in Section 2.2: The LIS was modified by adding a phosphor layer on the input area to sensitize it to x-rays. The deviation between the light and radiation field edges was calculated through a dedicated script operating on the unprocessed edge-file data. These were obtained using the software supplied by the hardware manufacturer of the LIS board. Curve fitting techniques were applied to the acquired edges and the mathematics is described in greater detail in the Appendix. To evaluate the different choices of phosphor thicknesses and particle sizes available to modify the sensor, some were tested on the early prototypes. To evaluate other hypothetical variants, a model was used to generate outcomes from more particle and phosphor thickness combinations. This modeling procedure is described in the Appendix. Assessment of the fully developed LIS-method (device and software) is described in Section 2.3 together with a comparison to three existing methods/devices in Section 2.4. All uncertainty calculations and terminology is based on the Guidance to the Expression on Uncertainty in Measurements (GUM).[11]

2.1 The fields and their edges – a short overview

The definitions of field edges (either light or radiation field edges) have proved to be non-trivial. The International Electrotechnical Commission (IEC 2009)[6] clarifies the *radiation field* as follows: "the boundary of an x-ray field is described as the locus of points at which the air-Kerma rate is 25% of the mean of the air-Kerma rates at the approximate centers of the quarters of the area enclosed".

Furthermore, the Food and Drug Administration (FDA 2012)[12] defines the *light field* as: "Light field means that area of the intersection of the light beam from the beam-limiting device and one of the set of planes parallel to and including the plane of the image receptor, whose perimeter is the locus of points at which the illuminance is one-fourth (25%) of the maximum in the intersection". The number within the brackets was added by the authors of this work for clarity.

Hulthén (2013) concluded that 25% of the maximum luminance of the light field is the closest to the apparent edge as perceived by an observer.[13] This is also in agreement with the definitions of the diagnostic field boundaries[11]. However, the encountered edge definitions in diagnostic radiology, do not overcome the obstacle of blurred edges as well as varying gradients. The standard approach to edge detection, where edges are defined as discrete steps in intensity changes, fails to reliably detect and localize edges in natural images where blur scale and contrast can vary over a wide range.[14] A blurred edge can then instead be described using so called Sigmoid functions.[15,16] This curve fitting method is described in greater detail in Appendix.[17-19]

2.2 The LIS method – development process

The developed LIS-method is of a field edge measuring type and is based on boards originally designed for light spectrometry.[20] The boards used are equipped with Toshiba 1204, 1304 or Hamamatsu (CMOS) 11639-01 linear sensors. The sensor acquires a 1D image (i.e. profile) of the edge projected on the LIS for further software analysis using a simple USB connection to a PC. For later prototypes, a Wireless Bluetooth connection (100 m version) have been added as an option to increase flexibility and avoid the impracticality of cables.

The sensor is sensitized to x-rays by applying a strip on its entire light entrance area using a well-known polycrystalline (powder) phosphor: Terbium activated Gadolinium Oxysulphide, (Gd_2O_2S:Tb).[21,22] Even though the LIS sensor is fully covered, the strip is still transparent enough for the sensor to monitor the light impinging on it when checking the light field. The developed LIS-

method can therefore localize the edges of both field types in the same sensor and hence estimate their congruence.

A unique feature of the LIS is its high resolution due to the small pixel size of (W×L) 200 μm×8 μm. Total sensor length is between 2.5 to 2.9 cm, depending on type used. This is more than sufficient for most misalignments and penumbras encountered in x-ray fields. The LIS is controlled as a camera sensor, in part utilizing the graphical user interface (GUI) software usually provided by the board manufacturer. The GUI software installs and runs under Microsoft Windows and is essential for the
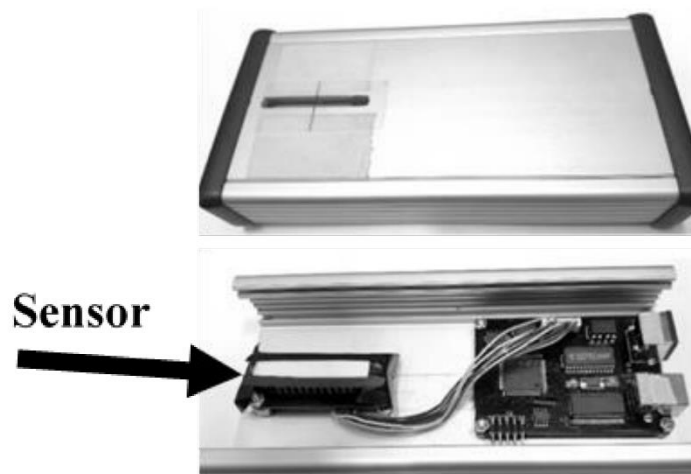

Fig. 1 One of the prototype versions of the LIS device in this work. (Top) Assembled. (Bottom) showing LIS connected to main board comprising a USB connection for further profile analysis on a PC. Phosphor strip on sensor is clearly seen in this picture.[13]

retrieving and storing of the edge profile. The software can set various acquisition parameters for the LIS-device, such as maximum recordable exposure time, number of consecutive exposures stored by the LIS etc. Furthermore, external or internal trigger and storage space can be selected. The most recent hardware, allowing for external auto-triggering, eliminates the need for manual capture of the radiation field edge during an exposure. This was a drawback of the early prototypes. The LIS-systems 16-bit analog to digital converter (ADC) provides a signal dynamic range suitable for most

luminance situations and its available exposure time interval of 0.1 – 3500 ms makes it suitable for most x-ray applications. A simple user interface, combining the GUI and in-house programmed scripts, has been developed in order to optimize the board for its intended use in QC.

Optimizing the final radioluminescence signal level of the sensor also involves modeling variations in thickness and particle sizes of the phosphor strip (see Appendix).[23,24] A thicker phosphor means a higher sensitivity (attenuation of more x-ray photons and hence a higher light output). There is a trade-off, resulting in a lower resolution due to increased light diffusion between the point of emission and the phosphor exit surface. There is also a limit to the layer thickness beyond which the light output will no longer increase. Furthermore, enough light from the light field must be transmitted through the same phosphor layer, to detect the light field edge.[23,24]

There were phosphor strips available of 7 µm particle size and 100, 200 and 300 µm thicknesses. For a 25 µm particle size, a 100 µm thickness was available. In practice, this latter strip came closest to fulfilling the requirements of a working phosphor-sensor combination and was therefore used throughout this work. To allow for an adequate transmission of the light field, the customized phosphor layer had no reflective backing, such as is often encountered in intensifying screens and for instance used in one of the methods compared in this study: the RTI Visi-X[25] (see also Section 2.4). When the device is placed across a light- or radiation field edge, the edge profile is displayed in real-time in the graphical user interface (GUI) and is then stored by the user. The height of the profile can be adjusted prior to the acquisition by changing the sampling time and gain of the LIS.
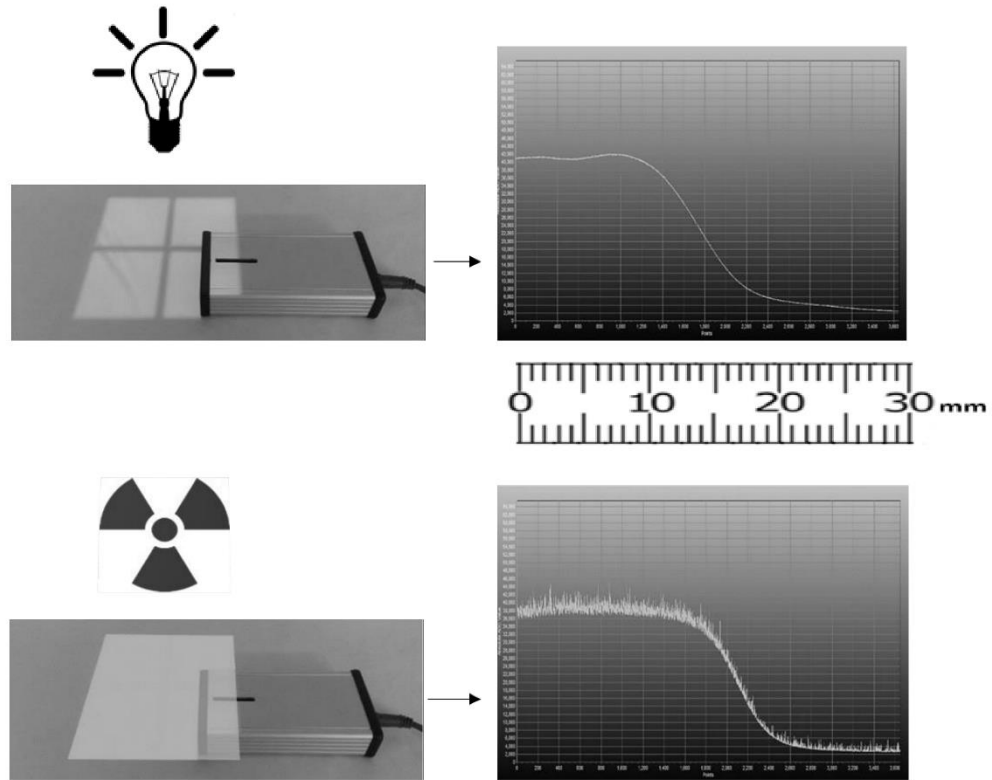
Fig. 2 Acquisition of the respective field edge profiles using an early LIS prototype.

(Top) The device in place with the slit perpendicular to the edge of one of the four sides of the light field and the profile appears in the GUI. A 1D image of the profile is stored. Field size 20 x 20 cm.

(Bottom) Without moving the device, an x-ray exposure is made and the 1D image of the radiation field edge profile is stored for one side at a time. The x-ray field is illustrated with the superposed square, not normally visible. Note the noise in x-ray field edge profile (lower right)[13].

The acquired light and radiation field edge profiles are read into a dedicated software to obtain the respective 25% levels. To improve the curve fitting procedure for the estimation of the 25% level, the edge profiles are processed to minimize the noise. For the light field edge profile, a gaussian smoothing is applied, the noise assumed randomly distributed (taking the average using adjacent values in the profile).

The conditions are different for the radiation field edge profiles, as they contain an additional noise component originating from x-ray photons interacting in the LIS, after passing through the phosphor layer. The result is a positive noise component to the profile, manifested as spikes superimposed onto the baseline signal from the phosphor (see Figures 2 and 3). The spikes must be removed prior to any further processing, otherwise the 25% level will not be found. This is accomplished by sliding an

eight-pixel wide window filter along the profile. The filter operates by adjusting the detected

maximum pixel value to the mean pixel value within the window. The spikes are then effectively

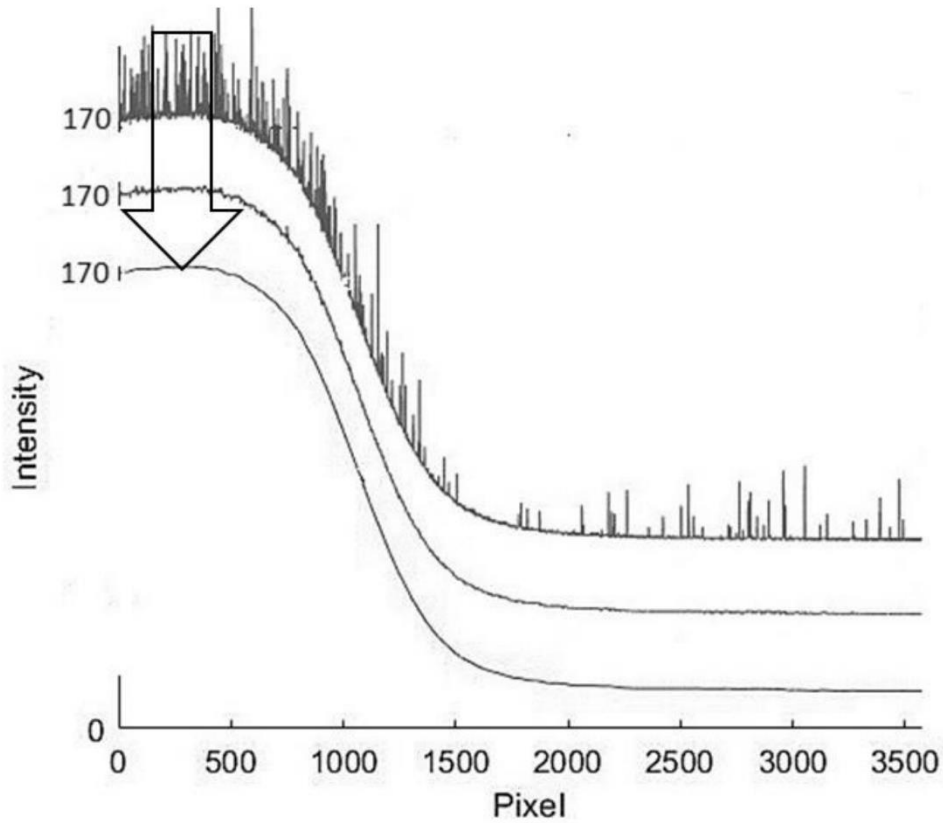suppressed while still maintaining the baseline signal level.[13]

Fig. 3 Illustration of noise suppression process. radiation field edge profile; before (top) and after (bottom) applying a positive noise suppression filter. An eight-pixel window slides across the profile replacing the maximum pixel value within the window equal to the calculated mean pixel value in the very same window. The spikes are effectively removed without altering the baseline of the profile. The remaining noise is assumed random and a Gaussian filter has been applied on the intermediate profile to remove the random noise before a 5PL-function (see Appendix) is finally fitted to the bottom noise processed edge profile.

The remaining noise is treated as random and gaussian filtering is applied in the same manner as for

the light field edge profile. Five-parameter logistic curves (described in Appendix) are then fitted to

the edge profiles to obtain the 25% points. Finally, the 25% intensity point location (pixel address) is

established for the light and radiation field edge profile respectively, and the difference between them

calculated. The difference is converted and finally presented in mm (see Figure 4)
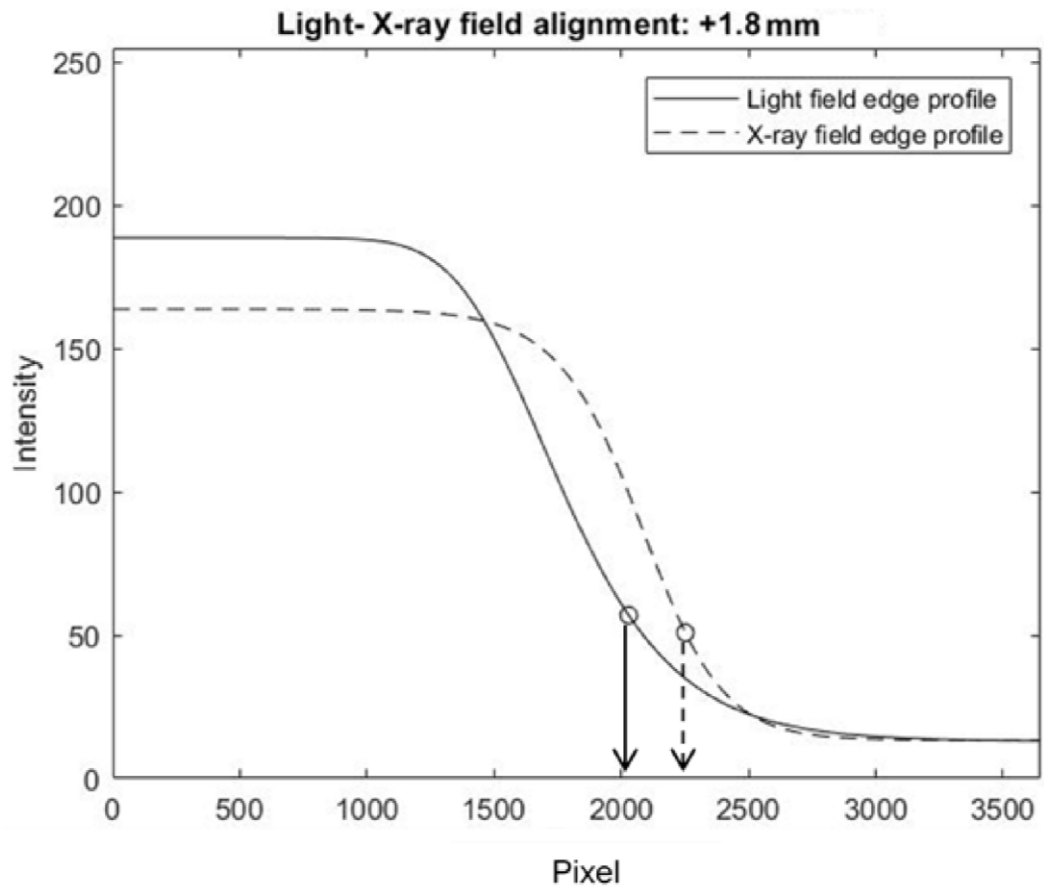
Fig. 4 The 25% edges of each profile, indicated by circular dots, (light field and radiation field) are compared and the difference in localization is converted to millimeters producing the alignment. In this example there is a deviation of +1.8 mm between the light field and radiation field edges

.

2.3 The LIS method – assessment procedure

Light field edges (Figure 2, top) were assumed to be stable due to the inherent, non-varying properties of the light sources.

However, during the planning of the assessment procedure, some initial testing of the radiation field edges indicated that an expanded assessment procedure was needed due to the unplanned encounter of a seemingly random change in localization. This was later identified as so-called focus spot wandering, further explained in Sections 3 and 4.[26] An intra-exposure edge localization series, i.e. several images (frames) taken during one single exposure, was therefore added for radiation fields. Any deviation outside of the inherent standard deviation is thought to be due to external factors, such as focus spot wandering.

The resulting properties of the sensitized sensor performing in a radiation field (Figure 2, bottom) were not known beforehand and the sensitizing phosphor, $Gd_2O_2S:Tb$, has a known energy dependence in the radiologic energy range. The potential influence on the LIS method results was therefore assessed by varying the tube voltage (kV_p). Air kerma dependence of the method was investigated by varying the mAs. For each profile, the edge location was determined and a deviation from the mean edge location value was then calculated.

2.4 Comparison to existing methods
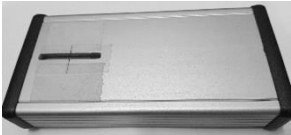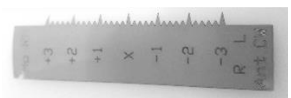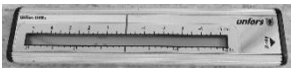
The method was compared to three other established methods for the light field radiation field congruence. All methods were compared and tested at the Karolinska University Hospital's research facility on the same diagnostic x-ray equipment.

An assessment of the various settings needed for comparable methods was also carried out. Finally, the total uncertainties of the LIS method and other methods were determined. The compared methods/devices were:

1) Gafchromic film (XRM2); a filmstrip increasing darkness with dose – field edge method[27]

2) Raysafe (DXR+); an electronic ruler consisting of a photodiode array displaying results on LCD scale – field edge method[28]

3) RTI Electronics (Visi-X), a phosphorescent plate showing the radiation field as an afterglow in a screen – full field method[25]

Table 1 Compared methods/devices

Method/device Commercial name, Method Type, Sensor	Light field edge position determined manually	Storing results electronically for later analysis	Estimated deviation shown directly without additional processing	Image of device (not in scale)	Overall size (mm)	Sensor /Detector size (mm) L x W
LIS-method Field edge, x-ray sensitized LIS	Not necessary	Yes	Yes, calculated deviation between field edges displayed directly in mms. Manual read-out eliminated.		160 x 72	29 x 0.08
Gafchromic film (XRM2)[27.], Field edge, Radiochromic film	Yes, essential	No, but can be used as a permanent record	No, scale indication through color tone change. Manual readout necessary.		89 x 25	89 x 25
Raysafe DXR+[28], Field edge, Photodiode array	Yes, essential	No	No, indication in LCD scale. Manual readout necessary.		30 x 145	100 x 2.5
RTI Electronics Visi-X[25], Full field, Phosphorescent screen	Yes, essential	No	No, afterglowing radiation field position in screen with scales. Manual readout necessary.		276 x 320	220 x 220

3 Results

3.1 Edge localization assessment

The edge localization dependence tests for the radiation field were executed by varying generator settings. Results were automatically stored and evaluated. The tests were in turn: Repeatability (keeping all parameters fixed), varying the kVp while keeping all other parameters fixed and mAs change (remaining parameters fixed). Typical results are shown in Fig. 5 for mammographic and

conventional x-ray systems. An initially unexplained systematic localization shift was observed and found to be independent of any settings of the x-ray equipment and LIS device. The unexpected shift was finally identified as a focal spot wandering effect due to thermal expansion of the anode rod (see Discussion Section). This effect is not noticed in the other compared methods due to their lower inherent spatial resolution (see 3.3). The results from the conventional x-ray system are from a series of acquisitions. Note the effect of a five minutes pause between the 5th and the 6th measurement during which the equipment had time to cool down
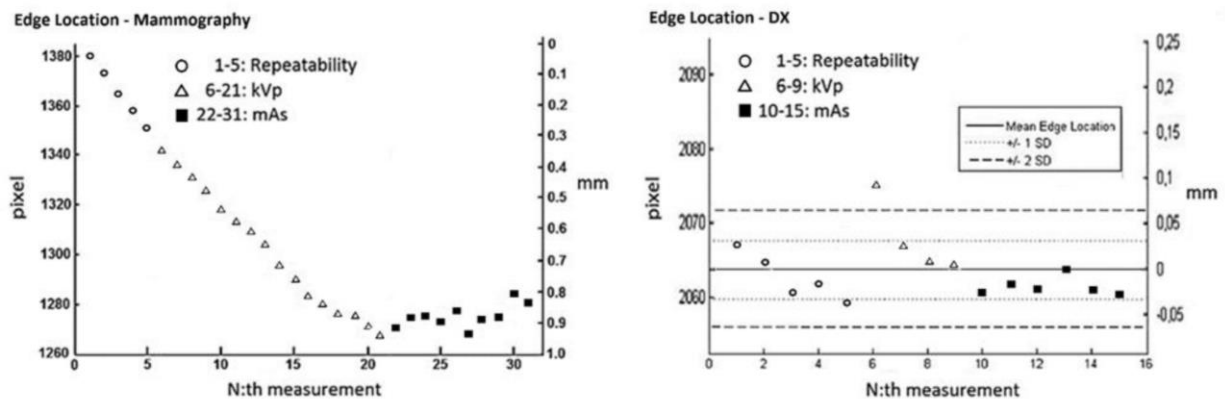

Fig. 5 Consecutive Edge Location results for varying settings. x-ray edge location mammographic equipment (left). 1 pixel = 8 µm. Apparent focal spot wandering is shown (see text for explanation). x-ray tube is cold at starting point (#1). Thermal balance is achieved following approximately 15 exposures i.e. wandering effect ends. Settings:1-5: 28 kVp/50mAs, 6-21: 25-34 kVp/50 mAs, Rh-filter and 22-31: 28 kVp/40-200 mAs. Edge location results for conventional-system (right). Apparent focal spot wandering is observed. x-ray tube cold at starting point (#1). Allowed to cool between exposure #5 and #6. Settings: 1-5: 80 kVp/50 mAs, 6-9: 60-100 kVp/50 mAs, 10-15: 80 kVp/20-100 mAs.

Results of intra-exposure variation measurement is shown in Table 2 for radiation field edge. Tests also confirmed the prior assumption on the light field i.e. the edges were stable throughout all measurement series and was on par with the intra-exposure measurements on radiation field edges or better. The light field edge location variations were therefore not further investigated, and the results are not presented here.

Table 2 Inherent uncertainty of the radiation field edge determination of the LIS method. Results from an intra-exposure variation measurement were in total five frames were captured during one x-ray exposure. Edge location (25%) was determined for each frame (profile). The equivalent pixel number, their mean and standard deviation, of the sequence is presented. Pixel number SD ~19 µm (1 pixel = 8 µm)

Nth frame	1	2	3	4	5		
Edge Location							
Pixel number (calculated)	2071,5	2075,4	2072,1	2069,6	2074,6		
					Mean:	2072,6	
					SD:	2,36	

3.2 LIS method uncertainty

The uncertainty is calculated following the recommended process of GUM[11]. There are two sources

of uncertainty in the localization of the light and field edge respectively, both characterized as *type A*

uncertainties. Firstly, two images of the same field edge are not perfectly identical due to e.g. noise

(statistical, electronic and fluctuations in output). The standard deviations of the intra-exposure

measurements described in earlier Section, were estimated as $\alpha = 23$ µm for the light field and $\beta = 19$

µm for the radiation field (see Table 2).

A second source of uncertainty is due to the difference in pixel location between the measured (and

noise filtered) field edge and the final fitted curve edge. The standard deviation of this difference was

calculated as $\gamma = 26$ µm for the light field and $\delta = 16$ µm for the radiation field. The expanded

uncertainty (coverage factor $k = 2$) for the determination of the light-radiation field congruence was

then determined to be 85 µm, i.e. from $\sqrt{\alpha^2 + \beta^2 + \gamma^2 + \delta^2} = 42,7$ $(k = 1)$.

Another possible uncertainty source is any angular deviation from the requirement of placing the LIS

perpendicular to the light field edge. In practice, an angular error smaller than about 10 degrees was

normally achieved, introducing a maximum error of $\cos^{-1}\theta$, i.e. about 1,5% and therefore considered

negligible.

3.3 Comparison to existing methods; dose requirements, congruence results

The lower limits of the air kerma required for an x-ray edge profile with the LIS device, are

determined by the combination of the phosphor strip x-ray to light energy conversion efficiency and

the light sensor sensitivity. Modelling several combinations of particle size and thicknesses of the phosphor strip (see Appendix) and functional tests of the strips available, resulted in the choice of a 100 µm thickness and 25 µm particle size. Theoretically, there are combinations that will produce even more light from the phosphor strip, but these were not available in practice and layers of greater thickness would inevitably lower the transmitted luminance from the light field. The minimum air kerma required was calculated to be around 1 mGy for both mammography (29 kVp, 20 mAs, W/Rh-filtration) and conventional x-ray system (70 kVp, 25 mAs). This is lower than the calculated minimum values for the other devices in the comparison: Gafchromic film; 12 mGy. RTI Visi-X (mammography and conventional); 15 mGy. Raysafe DXR+; 2 mGy and 12 mGy (mammography and conventional).

The Visi-X and Gafchromic film method may at occasions need several exposures due to the relatively low exposures from some dental and mammographic x-ray equipment. In the case of the Raysafe DXR+, the manufacturer recommends a tube current >100 mA and an exposure time >10 ms (i.e. >1 mAs). In practice, these settings did not deliver a sufficient exposure for the device to trigger. In mammography, the device did not respond at air kerma levels below those stated above.

The four methods produced consistent results within their calculated uncertainty ranges, displaying the same magnitude and sign. Results are presented for the same side/edge of the field(s) (see Table 3). Uncertainty estimates are from the work of Hulthén.[13] The exposure values were set according to the manufacturers' recommendations (or higher where necessary).

Table 3 Results – Light-radiation field congruence. +/- refers to the radiation field edge location relative to the light field edge location and + is outwards from the center of the field

Method:	LIS-method	Gafchromic film	RTI Visi-X	Raysafe DXR+

| Field edge | +1.76 mm | + 2 mm | + 2 mm | + 2.5 mm |
| Uncertainty | +/- 0.09 mm | +/- 0.5 mm | +/- 0.5 mm | +/-1.25 mm |

Discussion

The LIS method field edge profiles and their corresponding edge locations are obtained with a high accuracy (expanded uncertainty <0.1 mm) which is a notable improvement compared to existing methods (Table 3). Furthermore, the LIS method is the most sensitive instrument in the comparison, i.e., to assess the congruence, the sensor requires lower exposure in terms of air kerma for the radiation field edge.

The reason for the high sensitivity is the combination of the LIS and the optimized phosphor layer. A Gd_2O_2S:Tb phosphor strip of 100 µm thickness and 25 µm particle size was used in the most sensitive LIS prototype version. The final choice of phosphor layer was based on the requirement to increase the sensitivity to x-rays of the LIS method and still be able to detect the light field through the semi-transparent phosphor layer (with no reflective backing layer).

A simple model for estimates of suitable phosphor layer properties[23,24] was used at a later stage in the development process: see overview in Appendix. The model predictions for a variety of available phosphor layer characteristics show a peak light energy for the LIS method at about 200 µm for 25 µm particle size and 100 kVp x-ray generator setting. However, the 100 µm phosphor strip used in the prototype proved adequate in practice. Even if the modelling results showed that there is potential for an even higher sensitivity to x-rays, the LIS method already has a high sensitivity compared to other methods evaluated in this work. Nevertheless, the model gave a useful hint for future design developments.

The calculated congruence of the LIS method agreed with those obtained using the other, commercially available methods (tables 1-3). The expanded uncertainty of the edge location of the LIS-method was estimated to be 0.086 mm which is considerably less than that of the other methods. It should also be noted that the Raysafe DXR+ device has a too large an uncertainty to be useful when

checking the x-ray overshoot on the breast support edge in mammography[7] (a maximum +2 mm overshoot from support edge is allowed according to IEC standards).

During the research and development process of the LIS method, it was noted that the radiation field edge position under observation would change slightly between exposures. As far as the authors know, this is the first time were focal spot wandering of x-ray equipment has been encountered and at the same time been quantified through measurements. This is a sign of the high-resolution capabilities of the method. Figure 5 shows how a mammography x-ray field edge moves up to 0.9 mm due to focal spot wandering, while it is less pronounced on conventional x-ray equipment. However, in general, this effect is thought to have negligible effect on image quality. An estimate of the magnitude of focal spot wandering comparable to our measurements, was not found in previously published literature. The phenomenon occurs mainly due to the temperature increase in the anode resulting in an extension of the anode rod (which is usually made of copper). The anode rod extension is believed to account for 75-80% of the focal spot wandering.[26] Manufacturers Siemens and General Electrics (GE)[29] confirmed that the measured field edge moving distance per exposure reported here seemed reasonable. Nearly a 100 μm/exposure shift can be expected on a cold x-ray tube. A Fujifilm engineer performing annual maintenance service on mammographic x-ray equipment stated further that the focal spot shift is accounted for by intentionally offsetting the radiation field approximately 1 mm at the chest wall edge.[29] It was shown that the edge moves following an exposure and not during the exposure itself, thus it is thought not to interfere with the image quality. However, this has not been investigated further.

A limitation of the LIS method is the requirement of four measurements for an entire field. At the moment there are technical limitations preventing the use of four LIS devices at once. This may change in the future. Another limitation is the susceptibility to cross-hairs in some light fields. The LIS should not be positioned in the shadow of a light field cross-hair. Other impacting factors on the light field edges are scratched or dirty panels in the collimator housing. In practice, it has to be a

significant number of scratches before any degrading in the light edge localization is noticed. Defects like these are also normally routinely discovered by the laboratory personnel.

For the x-ray field edges, there is an upper limit for the detectable congruence deviation, restricted by the length of the sensor, i.e. 29 mm. Consequently, if the LIS is put unintentionally outside the x-ray edge limit (but within the limit for the light field edge), no x-ray edge will appear. This could be an indication of a too large a deviation or that the light field edge has been detected very close to the physical limit of the sensor. To obtain a deviation figure, the device is simply moved closer to the position of the assumed radiation field edge and a new light field edge is acquired.

4 Conclusions

In this work the development of a new device for the estimation of the light field - radiation field congruence has been presented. It is a high resolution, Linear Image Sensor sensitized to x-rays by adding a selected phosphor converting x-rays to light on top the LIS camera. The developed LIS method estimates the light and the radiation field locations by their edges without the necessity of precise manual positioning prior to measurements, eliminating possible observational bias otherwise present in the alignment process of comparable methods. The LIS method was shown to have an expanded uncertainty of 0.09 mm in field congruence, fulfilling demands on congruence checking devices following from QC standards. A comparison was made with established devices. The uncertainty of the LIS method was concluded to be lower than for the comparable methods presented in this work. Furthermore, the device stores the light field and x-ray field profiles and from these, the congruence is automatically calculated. This eliminates the need for manually keying in the information to a spread sheet or similar, mitigating the associated risk for errors. The basic concept of the LIS-method also provides a platform for future developments for CT and Therapy accelerators.

Appendix.

The Sigmoid function and curve fitting to real edge profiles

Encouraging studies have been made where Sigmoid functions were fitted to radiation field penumbras.[13,14,16] We decided to use a Sigmoid type called Five Parameter Logistic function (5PL) (cf. equation 2) defined by its five variables. By defining the background intensity as *a* and the field intensity as *b*, a blurred edge can be expressed by the function *f(x)* such as

$$f(x) = a + \frac{b-a}{(1+e^{-\frac{(x-c)}{d}})^{1/E}}$$ (2)

The two parameters, *a* and *b*, are the asymptotic values when $x \to -\infty$ and $x \to +\infty$ respectively. Altering *c* shifts the transition region between the two asymptotes along the *x* direction. The fourth parameter *d* is a slope factor that determines the width of the transition region (Fig. 7).[16]
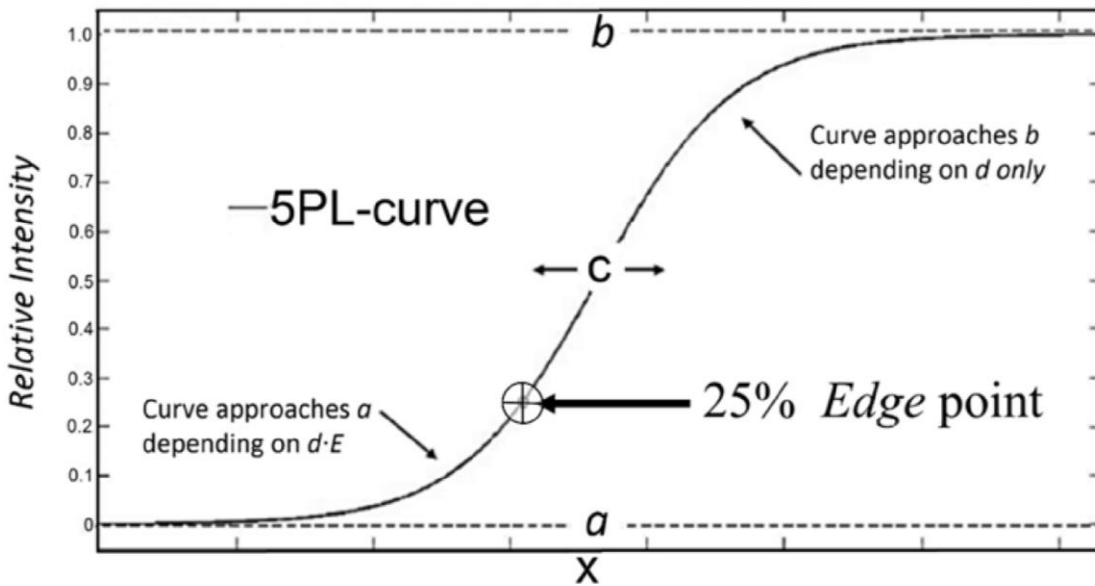
Fig. 6 A 5-parameter logistics curve. Parameters *a* and *b* are the asymptotic value when $x \to -\infty$ and $x \to +\infty$ respectively, parameter *c* shifts the curve in the *x*-direction. Parameters *d* and *E* dictates the near-asymptotic behavior of the curve. The 25% intensity value is indicated, i.e. the edge of the curve. Based on a figure from Hulthén (2013).[13]

The fifth parameter, *E* (> 0), rules the near asymptote maximum growth. If omitted (i.e. *E* = 1) the curve has its point of inflection (the point where the curve's concavity changes), and is symmetrical

around, *c*. Hence, when introduced it is thought to provide a closer fit to the field edges obtained clinically.

Mathematically it can be shown that parameter *d* controls the rate by which the 5PL curve approaches asymptote *b* (i.e. when $x \to +\infty$) and the product $d \cdot E$ governs the rate by which it approaches asymptote *a* ($x \to -\infty$).[16] It can be shown that the edge location, (x_{25}), for the 5-PL (utilizing the 25% definition) is obtained through:

$$x_{25} = -d \ln(4^E - 1) + c \qquad \text{(rising edge, } f'(x) > 0) \qquad (3)$$

$$x_{25} = -d \ln\left(\left(\frac{4}{3}\right)^E - 1\right) + c \qquad \text{(falling edge, } f'(x) < 0) \qquad (4)$$

We thus now have a mathematical tool to describe the edges that are encountered in realistic clinical scenarios.

Modelling of the radioluminescent layer

It is known that luminescent polycrystalline layers of a particular phosphor and equal thickness but with varying particle sizes will produce varying luminance for the same incident energy fluence and hence changeable extrinsic efficiency.[23,24] We have used a discrete model where the optical concept is expressed by the extinction factor (ξ). The extrinsic efficiency, *N*, of a radioluminescent layer can be defined as the ratio of light energy per unit area of the layer surface, Λ, expressed in the photometric unit $cdm^{-2}s^{-1}$, to the incident x-ray energy fluence rate Ψ_0 (Wm^{-2}) of perpendicularly incident x-ray photons.

$$N \equiv \Lambda / \Psi_0 \text{ , (cd W}^{-1}) \qquad (5)$$

Using this model, various particle size and layer thickness combinations in a phosphor layer can then be used to predict efficiency for the same basic design and extinction factor. According to the model[23,24], the total light energy emitted per unit surface area resulting from an energy impartation of x-ray energy to the radioluminescent layer can be described

21

$$\Lambda = \eta \Psi_0 \left(exp\left(\left(\frac{\bar{\mu}}{\rho_c} \right) \frac{L}{n} \rho \right) - 1 \right) exp\left(-(n+1) \left(\frac{\bar{\mu}}{\rho_c} \right) \frac{L}{n} \rho \right) \Sigma_{i=1}^{n} exp\left(+ \left(\frac{\bar{\mu}}{\rho_c} \right) \frac{L}{n} \rho \cdot i \right) (1 - \xi)^i \qquad (6)$$

where η is the intrinsic efficiency, ρ_c (g cm^{-3}) is the packing density of the radioluminescent layer, $\overline{\mu/\rho_c}$ (cm^2 g^{-1}) is the average mass attenuation coefficient of the radioluminescent material (phosphor/scintillator) weighted over the energy spectrum of the fluence rate, Ψ_0, of the impinging x-ray photons, i is a discrete layer in a slab of the radioluminescent material, n is the total number of discrete layers, ξ is the light extinction factor and $L/n = \Delta L$ where ΔL is the thickness of the discrete sub-layer corresponding to the average phosphor particle diameter assuming perfect spheres stacked in a matrix configuration. The expression (6) is generic and assumed valid for any polycrystalline phosphor exhibiting fluorescence and represents the *Transmission mode*, i.e. the light energy emitted at the opposing side to the x-ray fluence entrance side (which is appropriate to this work).

Applying the presented model on the phosphor layer in this work provides projected signal level changes for various particle size thickness combinations. However, it should be noted that the phosphor properties will determine the signal level for *both* light field and radiation field. The qualities of the phosphor strip (25 µm) in this work is identical to a previously assessed phosphor layer in reference 23. The results for the Gd$_2$O$_2$S:Tb phosphor are shown in figure 8 for ξ = 8,5%, ρ_c = 3,7 gcm^{-3} (50% packing density), $\overline{\mu/\rho_c}$ = 8 cm^2 g^{-1} (100 kVp x-ray spectrum). The light output is normalized to the maximum light output of the curve obtained for 25 µm average particle size. The 100 µm thickness phosphor strip chosen in the current LIS-method prototype is indicated (arrow). A 7 µm particle size strip is included for comparison. Going from 100 to 200 µm in thickness (for the 25 µm particle size) increases the light output 58% which would be the maximum (optimum) for the transmission mode in this context. In practice, this increase in signal should then be compared and matched to the light field induced signal, striving to avoid too many manual setting changes between field types. It can also be deduced from the model results that virtually no gain would achieved when

using the 7 µm particle size strip and switching from 100 to 200 µm thickness. The signal level would theoretically also be approximately 33% lower than the signal calculated by the 25 µm / 100 µm combination.
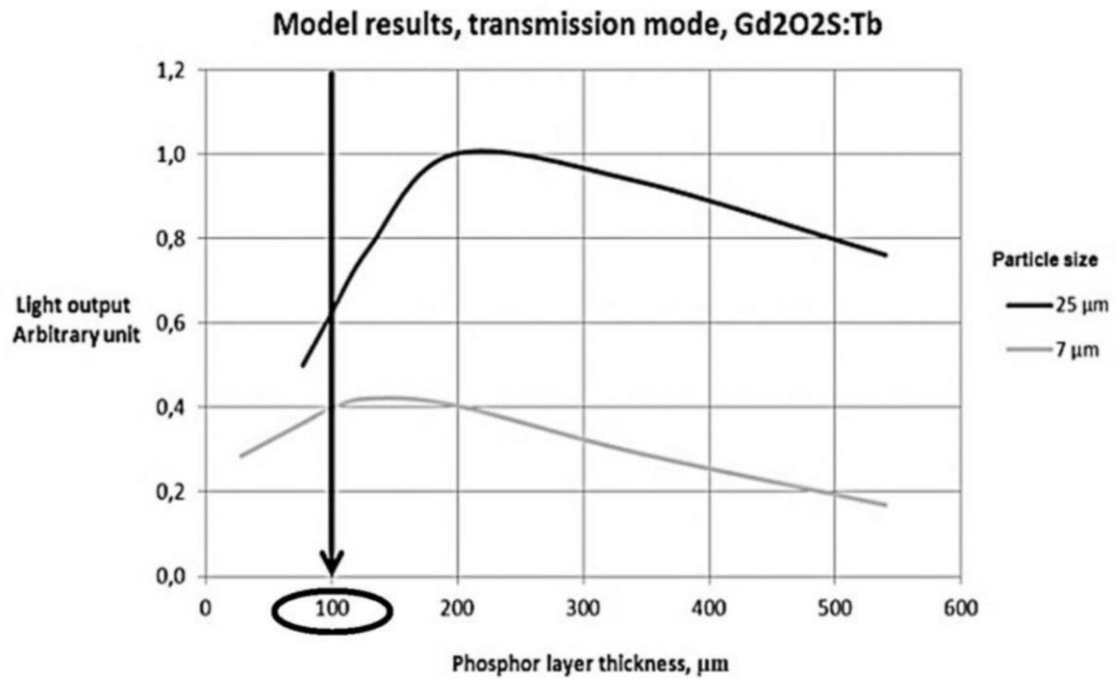
Fig. 7 Light output change in arbitrary units with increasing phosphor layer thickness shown for two particle sizes; 7 and 25 µm. The applied phosphor strip in the prototype is indicated in the diagram (25 µm particle size, 100 µm thickness). Arrow and encircled value indicate currently chosen thickness in the prototype.

Disclosures

The first author, Jan Lindström, reports that one of the commercial products subjected to a comparison in this work, Visi-X, was originally developed by him and is manufactured by his company Radicon, Sweden and marketed and distributed globally by RTI Electronics, Sweden.

References

1. Forster E., "*Equipment for Diagnostic Radiography*," MTP Press (1985).

2. Carlton R R., McKenna Adler A., "*Principles of Radiographic Imaging: An Art and a Science," 5th edition*. Delmar Cengage Learning (2012).

3. Fosbinder R A., Orth D., "*Essentials of Radiologic Science*," Lippincott, Williams & Wilkins (2011).

4. Walsh C., et al., "*Exposure variations under error conditions in automatic exposure-controlled film–screen projection radiography*", The British Journal of Radiology, 77, 931–933 (2012).

5. Lindström J., Karambatsakidou A., Short manuscript, "*Varying Light field – Radiation field congruence: PCXMC simulations for three clinical exam procedures*", Medical Physics Department, Karolinska University Hospital (2013). Available from jan.lindstrom@sll.se

6. International Electrotechnical Commission (IEC)., "*IEC 60601-2-54, International Standard, Medical electrical equipment – Part 2-54: Particular requirements for the basic safety and essential performance of x-ray equipment for radiography and radioscopy*", (2009).

7. International Electrotechnical Commission (IEC), "*IEC 60601-2-45, International Standard, Medical electrical equipment - Part 2-45: Particular requirements for the basic safety and essential performance of mammographic x-ray equipment and mammographic stereotactic devices",* (2011).

8. Kron T., Ferguson S., "*Where is the light field edge: perception of different operators on different surfaces*", Med Dosim. 25(2):99-103 (2000), doi:10.1016/s0958-3947(00)00036-4

9. Lindström J., et al., "*Optimizing two radioluminescence based quality assurance devices for diagnostic radiology utilizing a simple model",* Proc. SPIE 9033, Medical Imaging (2014): Physics of Medical Imaging, 90333R (19 March 2014); https://doi.org/10.1117/12.2042921

10. Bottaro M., et.al., *"Automated and observer based light field indicator edge evaluation in diagnostic X-ray equipment. Research on Biomedical Engineering"*, 33(2), 130-137. DC. (2017). https://doi.org/10.1590/2446-4740.07116

11. Guide to the Expression on Uncertainty in Measurements (GUM)., 2008, https://www.iso.org/sites/JCGM/GUM-introduction.htm

12. Food and Drug Administration (FDA)., *"Code of Federal Regulations, Title 21, Part 1020: Performance Standards for Ionizing Radiation Emitting Products"* (2012).

13. Hulthén M., *"Development and evaluation of a novel method for the control of the light field – radiation field congruence in diagnostic radiology"*, Master of Science Thesis in Medical Radiation Physics Stockholm University (2013). Available from markus.hulthen@sll.se

14. Hu X., *"Subpixel line extraction based on blurred edge model and adaptive least square template matching"*, ASPRS Annual Conference, Reno Nevada, May 1-5, (2006).

15. Hagara M., Kulla P., *"Edge Detection with Sub-pixel Accuracy Based on Approximation of Edge with Erf Function"*, Radioengineering, 20(2), 516-524 (2011).

16. Balderson M J., et al., *"Quality assurance using a photodiode array"*, Journal of Applied Clinical Medical Physics, 12(2), 191-200 (2011)

17. Wang H., Fallone B.G., *"A Mathematical model of radiation field edge detection"*, Medical Physics, 22(7), 1107-1110 (1995).

18. Ledvij M., *"Curve fitting made easy"*, Industrial physics, 9 (April/May), 24-27 (2003).

19. Gottschalk P G., Dunn J R., *"The five-parameter logistic: A characterization and comparison with the four-parameter logistic"*, Analytical biochemistry, **343**, 54-65, (2005).

20. Mightex OEM spectrometer by Mightex Systems https://www.mightexsystems.com/family_info.php?cPath=5_48&categories_id=48

21. Giakoumakis G E., Nomicos C D., Sandilos P X, *"Absolute efficiency of $Gd_2O_2S:Tb$ screens under fluoroscopic conditions"*, Phys. Med. Biol **34**, 673-678, (1989)

22. Yen W M., Shionoya S., Yamamoto H., (Editors), *"Phosphor Handbook",* CRC Press, Print ISBN: 978-0-84 93-3564-8, eBook ISBN: 978-1-4200-0523-3 (2006)

23. Lindström J., Alm Carlsson G., *"A simple model for estimating the particle size dependence of absolute efficiency of fluorescent screens"* Phys. Med. Biol. **44** (1999)

24. Lindström J., et al., *"Experimental assessment of a phosphor model for estimating the relative extrinsic efficiency in radioluminescent detectors"* Physica medica (Testo stampato), ISSN 1120-1797, E-ISSN 1724-191X, Vol. 76, s. 117-124 (2020)

25. Visi-X by RTI Electronics AB Flöjelbergsgatan 8 C SE-431 37 Mölndal, Sweden, http://www.rti.se/products/visi-x/

26. Stein A M., *"Analysis of a focus shift during the operation of an x-ray unit"*, The Russian journal of nondestructive testing, 48(6), 378-383, (2012).

27. Gafchromic film http://www.gafchromic.com/documents/PC-11805_Gafchromic_XR.pdf

28. Raysafe DXR+ http://www.raysafe.com/en/Products/Equipment/RaySafe%20DXR

29. Lindström J., Personal communication. *Discussion with representatives from GE, Fuji Film and Siemens,* Medical Physicist, Karolinska University Hospital, (2012)

First Author is a senior Medical Physicist at the Karolinska University Hospital. He received his Medical Physics degree from the University of Gothenburg, Sweden in 1986 and a licentiate from the University of Linköping, Sweden in 2011. His current research interests include phosphor modelling and new applications thereof.